Journal of Prime Research in Mathematics Vol. **4***(2008), 195-205*

MATHEMATICAL MODELING OF THROMBUS GROWTH IN MICROVESSELS

A. G. ALENITSYN*, A. S. KONDRATYEV**, I. MIKHAILOVA***, I. SIDDIQUE*,****

Abstract. Richardson's phenomenological mathematical model of the thrombi growth in microvessels is extended to describe more realistic features of the phenomenon. Main directions of the generalization of Richardson's model are: 1) the dependence of platelet activation time on the distance from the injured vessel wall; 2) the nonhomogeneity of the platelet distribution in blood flow in the vicinity of the vessel wall. The generalization of the model corresponds to the main experimental results concerning thrombi formation obtained in recent years. The extended model permits to achieve a numerical agreement between model and experimental data.

Key words: Mathematical model, microvessels, thrombi growth, platelets.

Aggregation of platelets at a mural site involves biochemical and physical processes, and the growth rates are affected by the neighboring flow field. Acute thrombogenesis in a flowing bloodstream occurs on damaged tissues in the normal circulation and the thrombi are composed predominantly of platelets. The reliable results of quantitative experimental data on growth rates of thrombi produced in vivo were obtained by Begent and Born [1], and the first theoretical description of the phenomenon was offered by Richardson [2] on the basis of the conception of "activation" time.

*Abdus Salam School of Mathematical Sciences GC University, Lahore, Pakistan.
**Herzen Pedagogical University of Russia, St-Petersburg, Russia.
E-mail: kondrat6125@mail.ru
***Pavlov Medical University, St-Petersburg, Russia.
****COMSATS Institute of Information Technology, Lahore, Pakistan.

Circulating platelets normally show no tendency to adhere to intact vessel walls, so a change must have come over those that adhere and aggregate where a vessel is injured. This change from a nonadhesive to an adhesive condition may usefully be referred to as platelet activation. Activation consists of different physical and biochemical events, for example, it is associated with an increase of free calcium in platelets [3]. The activation time of platelets is defined as the interval between the encounter of platelets with activating agents, such as ADP (adenosine diphosphate), and their ability to react with plasma fibrinogen [2,4]. According to modern representation [5] ADP opens calcium channels in the platelet membrane within 20 ms.

Richardson explained the main results obtained by Begent and Born. His theory depends on the assumption that platelets have a characteristic activation time. Evidence for the assumption was based on results obtained with the iontophoretic technique [6]. Thus, Richardson assumed a linear profile of blood flow velocity near the vessel wall with $\nu = \Gamma y$ (y is a distance from the damaged wall site in the direction perpendicular to blood flow; Γ is a velocity gradient near the vessel wall, which does not depend on y), and assumed the activation time t_A of 0.1–0.2 sec. independent of the distance from the wall. The expression obtained for the number of platelets aggregating per unit time is

$$N = \frac{2}{3} n_0 \Gamma R^3 F(\Gamma\tau), \tag{1}$$

where n_0 is a uniform platelet concentration per unit volume of blood, R is a radius of thrombus cross section in a direction normal to the blood flow, and $\Gamma\tau$ is a dimensionless parameter proportional to blood velocity: $\tau \sim t_A$. The function $F(\Gamma\tau)$ was shown to be:

$$F(\Gamma\tau) = \begin{cases} 1, & \Gamma\tau < 1; \\ 1 - \left(\frac{\sqrt{\Gamma^2\tau^2 - 1}}{\Gamma\tau}\right)^3, & \Gamma\tau > 1. \end{cases} \tag{2}$$

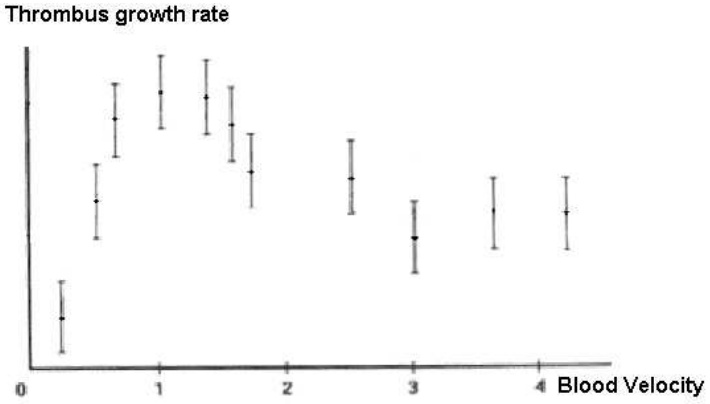

FIGURE 1. Mean growth rate of thrombus section in downstream direction as a function of mean blood velocity.

The comparison of experimental data of Begent and Born [1] and of Petrishchev and Mikhailova [7,8] (shown on Fig.1 in conventional units) with the Richardson model (1) (shown by the curve 1 on Fig.2) confirmed the basic idea of the activation time and indicated the necessity of the further development of the model which would take into account more realistic features of the phenomenon than those taken into account in deriving (1) and (2).

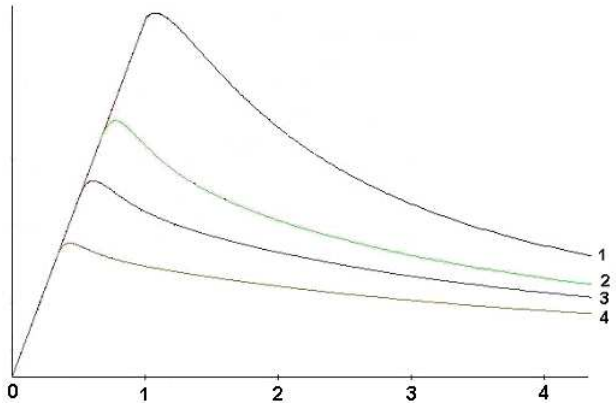

FIGURE 2. Model curves for the thrombus growth rate versus blood velocity.

A detailed discussion of the nature of the activation time [4,9] revealed ways in which the reaction time of individual platelets may be estimated from various experimental and theoretical approaches. The experimental determination of platelet activation time revealed several problems which had not yet been solved. One of the most important among them is whether the activation time is constant under varying conditions or may be altered by them. The chemical condition for platelet activation is the concentration of activating agents within and immediately around a growing thrombus. Thrombi can grow around a highly localized source of activating agent on the vessel wall. On the other hand, activation may be initiated through actual contact of arriving platelets with the thrombus. The transit time is not uniform for all platelets passing a thrombus, being shortest for those farthest from the vessel wall. As the shear rate increases with increasing blood flow velocity, the platelets more able to escape capture are those passing over the top of the thrombus rather than those passing its sides [9]. The concentration of activating agent decreases with the distance from the wall.

Thus, the most evident generalization of the Richardson model is associated with the assumption that the activation time t_A depends on the distance y from the damaged wall site [10]. Concentration of ADP decreases with the distance from the damaged site and consequently the activation time increases. The corresponding law can be assumed to be

$$t_A = t_{A_0} + \alpha y^k \tag{3}$$

where t_{A_0}=the activation time near the wall; k–is a phenomenological parameter of the model. The expression for aggregation frequency in this case is similar to Eq. (1):

$$N = \frac{2}{3} n_0 \Gamma R^3 F(\beta, \Gamma\tau), \tag{4}$$

where $\beta = \alpha R^k / t_{A_0} > 0$. Analytical expressions for $F(\beta, \Gamma\tau)$ can be obtained for several different values of k [7]. For the simplest linear dependance $k = 1$ we have

$$F(\beta, \Gamma\tau) = \begin{cases} 1, & \Gamma\tau(\beta+1) < 1; \\ 1 - \left(1 - \frac{1}{4\beta^2}\left(\sqrt{1 + \frac{4\beta}{\Gamma\tau}} - 1\right)^2\right)^{3/2}, & \Gamma\tau(\beta+1) > 1. \end{cases} \tag{5}$$

Further development of the model should be associated with considering rheological factors in platelet-vessel wall interactions which involve cell-cell encounters, platelet-vessel wall encounters and platelet-thrombus

interactions [9,10]. Among different factors that influence the process of thrombi formation one should take into account that thrombus growth rates are affected by the presence of red cells which are larger than platelets. The effect attributed initially to enhancement of platelet diffusivity by red cell motion was considered as a purely rheological effect, but later was considered to involve the red cell biochemically as well.

After different experimental investigations of the problem it became clear that experiments to test the hypothesis about the nature of the chemical response of red cells under shear are difficult to perform because the amounts of adenine nucleotides being looked for are rather small. The results do not yet appear definitive [11].

Animal models provided opportunities for observation of thrombus growth [12]. In the microcirculation (mouse mesentery, rat mesentery, rat cremaster, etc.) it was possible to record thrombus growth on an injured vessel site by using a $1\,mA$ discharge or a laser beam to induce vessel damage. The aggregometer and electron microscope showed how platelets are activated by an adequate concentration of ADP, with morphological changes leading quite rapidly to the development of pseudopodia. It was realized that the development of pseudopodia would increase the effective cell radius and thereby increase the collision frequency in a shear flow. The discussed and other observations lead to a thrombosis hypothesis incorporating feedback [9]. This hypothesis was formulated to give distinguish between processes that are predominantly physical or predominantly biochemical.

The study of the adhesion of platelets to foreign surfaces led to observation that many platelets depart after adhesions lasting 2-3 min, and moreover that sites previously occupied by platelets were preferred for adhesion by platelets (passing subsequently) compared with unused adhesion sites [13]. It is not yet clear whether repeated adhesions and detachments are necessary to augment the adhesiveness, or whether it occurs with the passage of time after a damaging event as illustrated by the results of [14].

Coming to the conclusion of this brief discussion we should state again that the magnitude of the forces that can be exerted between platelets and a wall are not well known, although this is obviously important in determining the stability of adhesion.

The experiments produced both in vivo and in vitro showed that platelet concentration profiles in flowing blood have excess concentration near walls [15–20]. The typical profiles of platelet concentrations in

vivo are shown on Fig.3 [20]. Concentration profile of blood platelets in vivo differs in arterioles and venules.

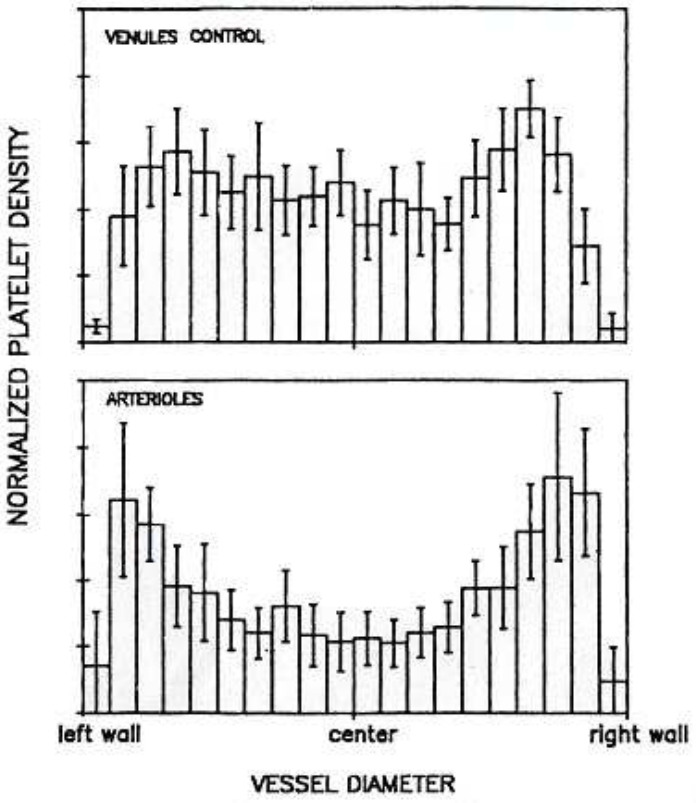

FIGURE 3. Experimental data for platelet concentration in venules and arterioles.

The model based on the extended equation for platelet transport was developed in [21]. The extended equation in [21] is a single component description, but it implicitly includes effects due to red cells and plasma by the use of an augmented diffusion constant and the drift function which is introduced to describe rheological events that are not encompassed by the use of an augmented diffusion coefficient. The transport equation was numerically integrated to determine concentration profiles. The calculated concentration profiles had near-wall excesses that qualitatively mimic experimental results, thus implying the extended equation is an adequate description of rheological events.

Once activated, platelets bind soluble adhesive molecules and become the reactive surface for continuing platelet deposition. Initial platelet tethering to a surface and subsequent platelet-platelet cohesion are typically identified as two separate stages of thrombus formation, defined as adhesion and aggregation, respectively [22]. Thus, at both early and late stages of thrombus formation, platelet adhesive mechanisms in rapidly flowing blood depend on multiple synergistic bonds, involving different receptors and ligands with specific functions [23].

In spite of considerable advances during the last several years, key aspects of the mechanism that regulate platelet functions in hemostasis and thrombosis remain to be elucidated. The interpretation of such findings, yet to be reported in full detail, may not be straightforward. Future research should offer a more global view of the processes underlying hemostasis and thrombosis. Thus, at the present moment we can consider only a phenomenological theory in describing the growth rates of thrombi.

Many factors described in the presented review of the phenomenon can be taken into account by the condition (3), so the most essential further generalization of the Richardson model is associated with the usage of a realistic profile of platelet distribution in the blood flow n(y). The qualitative estimation of the influence of the excess concentration made in [24] confirmed the advantage of such a model of platelet distribution. The same considerations that provided the derivation of the equations (1)–(5) lead to the following expression for the number of platelets aggregating per unit time:

$$N = 2R \int_0^{y_{max}} n(y)\nu(y)\cos\theta\, dy = 2R^3\Gamma \int_0^{\theta_1} n(\theta)\cos^2\theta\sin\theta\, d\theta, \qquad (6)$$

where $y = R\sin\theta$, $n(y)$ is a platelet concentration on the distance y from the wall, and all other notations coincide with those in (1) and (4). The upper limit of the integration is determined by the condition: if $\Gamma\tau(\beta+1) < 1$ then $\theta_1 = \pi/2$; if $\Gamma\tau(\beta+1) > 1$, then the limit θ_1 is determined from the equation:

$$\Gamma\tau\sin\theta_1(1+\beta\sin^k\theta_1) = 1 \qquad (7)$$

with $0 \le \theta_1 \le \pi/2$, where k is the phenomenological parameter in (3).

The present discussion leads to the conclusion that the generalized Richardson's phenomenological model taking into account the dependance of activation time on the distance from the vessel wall and real profile of platelet concentration in the blood stream is capable to present a proper quantitative description of the phenomena provided the parameters of the model can be varied in sufficient range. This requires a certain mathematical development of the model.

We start from the equations (1), (6) and (7), with the aim to construct a universal algorithm for plotting graphs of the function $\Gamma\tau F(\beta, \Gamma\tau)$ versus $\Gamma\tau$, applicable for any values of the phenomenological parameters $\beta \geq 0$ and $k > 0$ and for any reasonable choice of the function $n(R\sin\theta)$. To emphasize F we exclude N from (1) and (6); for $\Gamma\tau(\beta+1) \leq 1$, we get $F(\beta, \Gamma\tau) = 1$, while for $\Gamma\tau(\beta+1) > 1$, we get the expression

$$F(\beta, \Gamma\tau) = \frac{3}{n_0} \int_0^{\theta_1} n(R\sin\theta)\cos^2\theta\sin\theta\, d\theta, \tag{8}$$

with $\theta_1 = \theta_1(\beta, \Gamma\tau)$ satisfying (7). Note that $\sin\theta_1 = 1$ corresponds to $\Gamma\tau(\beta+1) = 1$.

Unfortunately, the equation (7) can be explicitly solved with respect to $\sin\theta_1$ for only several values of k, in particular, for the case $k = 1$ considered above. In the general case we will use the parametric representation of the mutual dependence between $\Gamma\tau$ and $F(\Gamma\tau)$.

For the sake of simplicity we take $R = 1$ and introduce the notations

$$x = \Gamma\tau, \quad y = xF(\beta, x), \quad p = \sin\theta_1, \quad 0 \leq p \leq 1.$$

The equation (7) takes the form $xp(1+\beta p^k) = 1$ and leads to the first parametric equation:

$$x(p) = \frac{1}{p(1+\beta p^k)}, \tag{9}$$

while (8) results in the second parametric equation:

$$y(p) = \frac{1}{p(1+\beta p^k)} \cdot \frac{3}{n_0} \int_0^{\arcsin p} n(\sin\theta)\cos^2\theta\sin\theta\, d\theta,$$

or, after the substitution $s = \sin\theta$,

$$y(p) = \frac{1}{p(1+\beta p^k)} \cdot \frac{3}{n_0} \int_0^{p} n(s)s\sqrt{1-s^2}\, ds, \quad 0 < p \leq 1. \tag{10}$$

Formulae (9)–(10) enable one to plot on the (x, y)-plane a graph of the desired function $y = \Gamma\tau F(\beta\Gamma\tau)$ versus $x = \Gamma\tau$, but only for values $\Gamma\tau(\beta+1) \in [1, \infty)$ which correspond to $0 < p \le 1$, or $\frac{1}{\beta+1} \le x < \infty$. In order to obtain a complete graph, the functions $x(p)$, $y(p)$ should be continued to the rest interval $p \in (1, \infty)$, which corresponds to $0 < x < \frac{1}{\beta+1}$. The continuation of $x(p)$ onto the range $p > 1$ is defined by the same formula (9); the function $y(p)$ is continued as $y(p) = x(p) = \frac{1}{p(1+\beta p^k)}$ because here $F(\beta, \Gamma\tau) = 1$.

In the simplest model, when n is taken as a constant $n \equiv n_0$, the integral (10) is easily evaluated, so for $0 < p < 1$ we have

$$x(p) = \frac{1}{p(1+\beta p^k)}, \quad y(p) = \frac{1}{p(1+\beta p^k)}[1 - (1-p^2)^{3/2}].$$

In the very special case $\beta = 0$ we get the Richardson model: $y = x(1 - (1 - x^{-2})^{3/2})$.

In more realistic models, where n is assumed to be variable, the scaling factor n_0 should be chosen in such a way that the resulting curve $(x(p), y(p))$ be continuous at $p = 1$. So we can write:

$$1 = \frac{3}{n_0}\int_0^1 n(s)s\sqrt{1-s^2}\,ds, \qquad n_0 = 3\int_0^1 n(s)s\sqrt{1-s^2}\,ds.$$

The ultimate parametric equations

$$x(p) = \frac{1}{p(1+\beta p^k)}, \quad y(p) = \frac{1}{p(1+\beta p^k)} \cdot \frac{I(p)}{I(1)},$$

with $I(p) = \int_0^p n(s)s\sqrt{1-s^2}\,ds$, are valid for $p \in (0, 1]$, while for $p \in [1, \infty)$, we have simply $y = x = \frac{1}{p(1+\beta p)^k}$.

With the use of mathematical computer packages (e.g., Maple or Derive), the proposed algorithm provides a very convenient way to plot graphs for various values of the phenomenological parameters.

The calculations show that the best agreement with the experimental data is archived when the parameter k in (3) equals 1 and the concentration of platelets $n(s)$ is approximated by the function

$$n(s) = 2 - \left((1.8s^2 - 0.3)^2 - 0.8\right)^2$$

shown on Fig. 4, which suits the experimental data for venules shown on Fig. 3 and corresponds to the results of [7,8].

The curves 2, 3 and 4 on Fig. 2 correspond to the values of the parameter β, equal 0.5, 1.0 and 2.0 correspondingly.

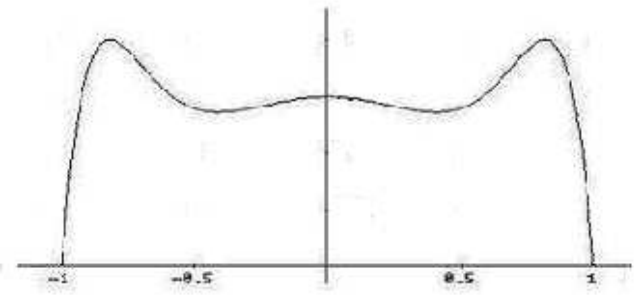

FIGURE 4. Model function n(s) for the concentration of platelets in venules.

It should be mentioned that the model proved to be stable relative small variations of all the parameters.

REFERENCES

[1] N. Begent, G. V. R. Born, *Nature,* **227**, 926 (1970).
[2] P. D. Richardson, *Nature,* **245**, 103 (1973).
[3] S. O. Sage, J. E. Merritt, T. J. Hallam and T. J. Rink, *J. Biochem*, **258**, 923 (1989).
[4] G. V. R. Born and P. D. Richardson, *Journ. Membrane Biology,* **57**, 87 (1980).
[5] A. Bonnefoy, Q. Lui, C. Legrand, M. Frojmovic, *J. Biophys,* **78**, 2834 (2000).
[6] N. Begent, *Ph.D. Thesis,* Univ. of London (1971).
[7] I. A. Mikhailova, *Sechenov Physiolog. Journ. USSR,* **77**, 95 (1991).
[8] N. N. Petrishchev, I. A. Mikhailova, *Microvascular Res.*, **49**, 12 (1995).
[9] P. D. Richardson , *Phil. Trans. R. Soc. Lond.*, **B294**, 251 (1981).
[10] A. S. Kondratyev, I. A. Mikhailova, N. N. Petrishchev, *Biophysics,* **35**, 469 (1990).
[11] G. V. R. Born, M. Kralger, *Revue Med. Brux.*, **2**, 157 (1981).
[12] B. Furie, B. C. Furie, *J. Clin. Invest.*, **115**, 3355 (2005).
[13] P. D. Richardson, S. F. Mohammed, R. G. Mason, M. Steiner, R. Kane, *Trans. Am. Soc. artif. intern. Organs.*, **25**, 147 (1979).

[14] I. A. Fenerstein, U. Marzeo, E. F. Bernstein, *Trans. Am. Soc. artif. intern. Organs.*, **26**, 172 (1980).
[15] P. A. M. M. Aarts, S. A. van den Broek, G. W. Prins, G. D. C. Kuiken, G. G. Sixma, R. M. Heethaar, *Artheriosclerosis*, **8**, 819 (1988).
[16] J. M. S. Pontius, *Thesis*, Univ. of Miami, Coral Gables, FL (1989).
[17] E. C. Eckstein, A. W. Tilles, F. J. Millero, *Microvasc. Res.*, **36**, 31 (1988).
[18] C. M. Waters, E. C. Eckstein, *Artif. Organs,* **14**, 7 (1990).
[19] R. E. Rumbaut, D. W. Slaff, *Burns Microcirculation,* **12**, 259 (2005).
[20] B. Woldhuis, G. Tangelder, D. W. Slaaf and R. S. Reneman, *Am. J. Physiol. (Heart Circ. Physiology),* **262**, H1217 (1992).
[21] E. C. Eckstein, F. Belgacem, *Biophys. J.,* **60**, 53 (1991).
[22] Z. M. Ruggery, *J. Clin. Invest.,* **105**, 699 (2000).
[23] S. Kulkarni, S. M. Dopheide, C. L. Yap, C. Ravanat, *et al*, *J. Clin. Invest.*, **105**, 783 (2000).
[24] A. S. Kondratyev, I. A. Mikhailova, N. N. Petrishchev, *Biophysics,* **43**, 115 (1998).